

# Generalisation of Event Turfs Decipherable Through HNA Process

K.Rekha <sup>[1]</sup>, Dr.K.Thirugnanasambandam <sup>[2]</sup>

Phd Scholar <sup>[1]</sup>, Assistant Professor <sup>[2]</sup>

Department of Mathamatics

Manonmanium Sundaranar University, Tirunelveli <sup>[1]</sup>

Govt Thirumagal Mills College, Gudiyattam <sup>[2]</sup>

Tamil Nadu – India

## ABSTRACT

A range of extensions to the HNA method are made in this paper. HNA methods for convex polygons use an approximation space on two overlapping meshes, here we use HNA on a single mesh. This single-mesh approach is easier to implement, and we prove that the frequency-dependence of the size of the approximation space is the same as for the overlapping mesh. We generalise HNA theory to provide a priori error estimates for a broader range of incident fields than just the plane wave, including point sources, beam sources, and Herglotz-type incidence. We also extend the HNA ansatz to include multiple obstacles.

In addition to the development of HNA methods, we also consider other ideas and developments related to multiple scattering problems. This includes the first (to the best knowledge of the author) mesh and frequency explicit condition for wellposedness of Galerkin BEM for multiple scattering.

**Keywords:-** BEM, HNA

## I. INTRODUCTION

To date, every version of the HNA technique has been developed for finding issues of plane wave incidence (as in Figure 1.2(a)). However, root incidence (see Definition 1.6(i) and Figure 1.2(c)) additionally happens oft in sensible applications. for instance, in acoustic modelling, most sounds originate from a supply point; a plane wave model is just applicable once the supply is much far from the scattering obstacle (a plane wave is also taken as a degree supply at infinity).

Moreover, a degree supply is a lot of physically realistic (than a plane wave) because it satisfies the radiation condition. maybe less ordinarily studied could be a generalisation of the purpose supply; the beam source (see Definition 1.6(ii), and Figure 1.2(d)), that the purpose supply is unclean on a line. Our interest within the beam supply is just part actuated by direct application; we tend to expect it'll even be helpful for repetitious multiple scattering versions of HNA BEM, that area unit mentioned concisely. we tend to are fascinated by scattering by a general Herglotz-type incident field and Figure 1.2(b) for Associate in Nursinging example with Herglotz kernel). like the beam supply incidence, solutions to such issues might not have as several immediate applications.

Instead, our motivation is nested within a bigger plan for finding multiple scattering issues. The Tmatrom technique of needs Associate in Nursinging approximation of the far-field pattern of diverging wavefunctions, that the Herglotz kernel are often written. therefore it's necessary to grasp such issues to develop HNA ways that area unit compatible with the Tmatrom technique.

## II. TO GENERALISE HNA METHODS TO A BROADER CLASS OF OBSTACLES

In this paper, we aim to generalise HNA methods to a broader class of obstacles, though controlling our attention to the case of the convex polygon  $\Omega$ . For each new  $x$

$$U_j$$

{.....}

$$\Gamma^+ \Gamma_j + \Gamma^- \mathbf{R}^2 \setminus U_j x_j$$

Figure 1.1: Example of a emblematic extension of a single side  $\Gamma_j$ , and the image of  $x \in U_j$  replicated in the inestimable line  $\Gamma^\infty_j = \Gamma^- \cup \Gamma_j \cup \Gamma^+_j$ , to create the point  $x_j \in \mathbf{R}^2 \setminus U_j$ . problem considered, we will derive a boundary illustration analogous to using a half-plane formulation, extending a single side  $\Gamma_j$  (of the boundary  $\Gamma$  of the convex polygon  $\Omega$ ) substantially in both directions to form the

boundary of the half-plane (see Figure 1.6 for example of an extension of a typical side).

Considering a single side  $\Gamma_j$  of a convex polygon  $\Gamma$ ,  $1 \leq j \leq n_\Gamma$ , we define  $\Gamma_j^+$  and  $\Gamma_j^-$  as the infinite extensions of  $\Gamma_j$  in the clockwise and anti-clockwise directions. Denote by  $U_j$  the (open) upper-half plane relative to  $\Gamma_j^+ := \Gamma_j^+ \cup \Gamma_j \cup \Gamma_j^-$ , such that the unit normal  $\mathbf{n}_j$  points into  $U_j$ . Finally, we define  $\mathbf{x}'$  to be the reflection of  $\mathbf{x}$  across  $\Gamma_j$ . Formally,  $\mathbf{x} = \mathbf{x}'$  when  $\mathbf{x} \in \Gamma_j$ , otherwise  $\mathbf{x}' = 6 \mathbf{x}$  satisfies  $\text{dist}(\mathbf{x}, \Gamma_j^{\infty}) = \text{dist}(\mathbf{x}', \Gamma_j^{\infty}) = \frac{1}{2}|\mathbf{x} - \mathbf{x}'|$  (see Figure 1.1 for a visual example).

We will make manifold uses of the following illustration from which states that for  $v \in C^2(U_j) \cap C(U_j)$  sustaining the Helmholtz equation (1.3) and the radiation condition, we have

$$v(\mathbf{x}) = 2 \int_{\Gamma_j^\infty} \frac{\partial \Phi(\mathbf{x}, \mathbf{y})}{\partial \mathbf{n}(\mathbf{y})} v(\mathbf{y}) ds(\mathbf{y}), \quad \mathbf{x} \text{ in } U_j. \tag{1.1}$$

We note that this illustration holds for  $v = u^s$  (the scattered field constituent of the solution to (1.4)–(1.6)) and holds for plane waves proliferating in direction  $\mathbf{d}$ , provided that  $\mathbf{d} \cdot \mathbf{n}_j \geq 0$ , i.e. proliferating out of  $U_j$ . Our illustration for the Neumann trace of the solution to (1.4)–(1.6) will characteristically be of the form

$$\partial u / \partial \mathbf{n}(\mathbf{x}) = \Psi(\mathbf{x}) + 2 \int_{\Gamma_j^+ \cup \Gamma_j^-} \frac{\partial^2 \Phi(\mathbf{x}, \mathbf{y})}{\partial \mathbf{n}(\mathbf{x}) \partial \mathbf{n}(\mathbf{y})} u(\mathbf{y}) ds(\mathbf{y}) \tag{1.2}$$

$$\frac{\partial \Phi(\mathbf{x}, \mathbf{y})}{\partial \mathbf{n}(\mathbf{x}) \partial \mathbf{n}(\mathbf{y})} = \frac{iH_1^{(1)}(k|\mathbf{x} - \mathbf{y}|)}{4|\mathbf{x} - \mathbf{y}|} = \frac{ik^2}{4} e^{ik|\mathbf{x} - \mathbf{y}|} \mu(k|\mathbf{x} - \mathbf{y}|)$$

This leads to the boundary representation (2.2), since  $\mu(z) := e^{-iz} \frac{H_1^{(1)}(z)}{z}$

2

see [16, eq. (1.6)].

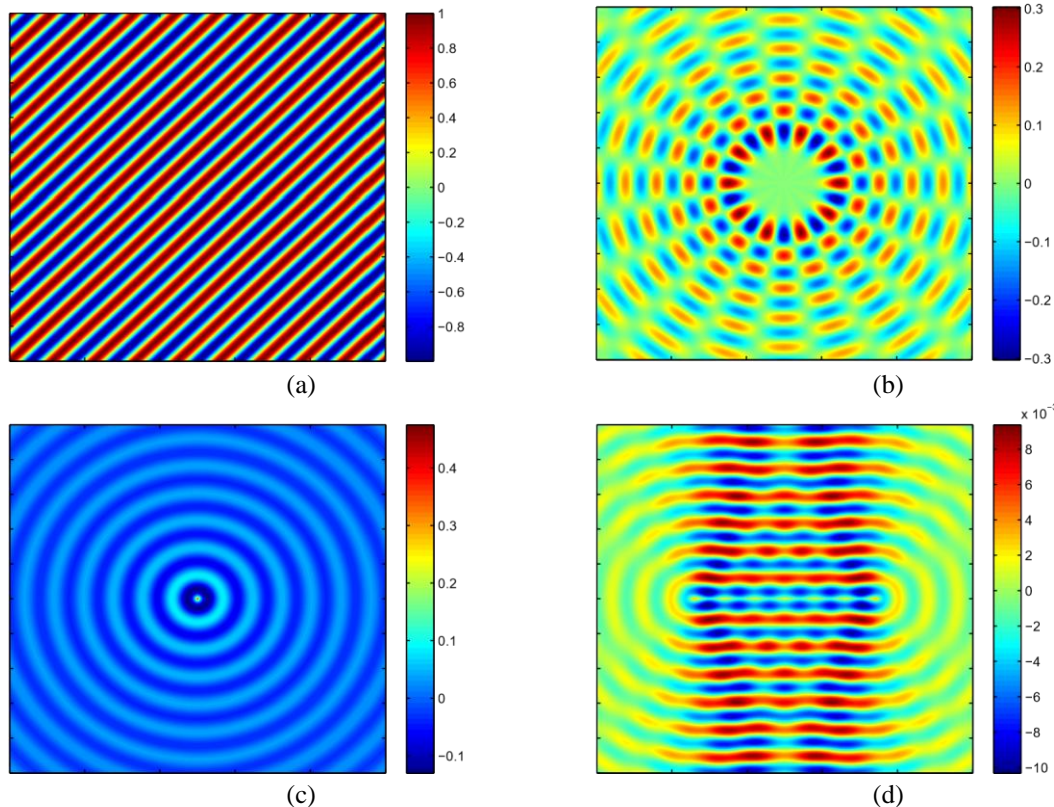


Figure 1.2: Examples of types of incident field solvable in this chapter, with wavenumber  $k = 40$  (although the wavenumber is irrelevant for (a) and (c)). (a) Plane wave. (b) Herglotz-type wave with kernel  $g_{\text{Herg}} =$

$-e^{-i\ell\theta}/(2\pi)$ . (c) Point source. (d) Beam source (see Definition 1.5) with  $\gamma = \{(x_1, x_2) \in \mathbb{R}^2 : x_1 \in [-1/2, 1/2], x_2 = 0\}$  and  $\varphi(\mathbf{x}) = 1/2 + x_1^2$ . As promised in Remark , we will generalise the definition of  $M(u)$  to problems where the incident field is unbounded at points inside the scattering domain  $\Omega_+$ . This definition will continue to depend on the size of  $u$  in some sense. We will conclude this introduction with a theorem which will be used in each problem considered in this chapter, and the multiple scattering problems. This theorem will enable us to bound the scattered field  $u^s$  in terms of the  $k$ -weighted norm of the incident field  $u^{inc}$  on the boundary  $\partial\Omega$ .

**THEOREM 1.1.** *For an obstacle  $\Omega_-$  with boundary  $\partial\Omega$  and incident field  $u^{inc}$  (in the sense of Definition 1.1), we have the following bounds on the corresponding scattered field  $u^s = u - u^{inc}$ , where  $u$  is the solution to (1.4)–(1.6): For star-shaped polygonal  $\Omega_-$  with boundary  $\Gamma = \partial\Omega$ ,*

$$\|u^s\|_{L^\infty(\Omega_+)} \leq C_1 \left[ \frac{p}{C_1 = \frac{5n_\Gamma / (8 \log 2) [1 + (2/\pi)(1 - \gamma_E + e^{1/4})]}{\text{essinf}(\mathbf{x} \cdot \mathbf{n}(\mathbf{x}))} \quad 2\text{diam}(\Omega)} \right. \\ \left. - \right) + \frac{1}{2k} \left] k^{-1/2} \log^{1/2}(2 + kL_*) \|u^{inc}\|_{H_k^1(\Gamma)}$$

where,  $\mathbf{x} \in \Gamma$

where  $n_\Gamma$  is the number of sides of  $\Gamma$ , whilst  $L_*$  denotes the length of the longest side and  $\gamma_E \approx 0.577$  denotes the Euler constant.

(i) More generally, for a non-trapping polygon  $\Omega_-$  with boundary  $\partial\Omega$ , given  $k_0 > 0$ ,  $k \geq k_0$ ,  $\|u^s\|_{L^\infty(\Omega_+)} \leq c k^{-1/2} \log^{1/2}(k) \|u^{inc}\|_{H_k^1(\partial\Omega)}$ , for  $k \geq k_0$ .

(Recall that  $a \cdot b$  is equivalent to  $a \leq cb$ , where  $c$  depends only on the geometry of  $\Omega_-$ .)

*Proof.* (i) We have the illustration  $u^s = -S_k A_k^{-1} f_k$  in  $\Omega_+$  (follows immediately from (1.10)), where  $A_k$  and  $f_k$  are As  $u^{inc} \in C^\infty(\mathbb{N})$  by, it follows that  $u^{inc} \in H^1(\Gamma)$ . Hence by the definition of  $f_k$ ,  $\|f_k\|_{L^2(\Gamma)} \leq \text{diam}(\Omega_-) \|u^{inc}\|_{L^2(\Gamma)} + k(\text{diam}(\Omega_-) + 1/2) \|u^{inc}\|_{L^2(\Gamma)}$

$$\leq \left[ \frac{1}{2\text{diam}(\Omega_-)} + \frac{1}{2k} \right] \|u^{inc}\|_{H_k^1(\Gamma)} \tag{1.3}$$

The result follows by combining (1.3) with the bound on  $S_k$  of [35, Lemma 4.1] and the bound on  $A_k^{-1}$  of [35, (4.5)] (noting that our definition of  $A_k$  is twice that of  $A_k$  in [52], as warned by Remark 1.5) with the bound

$$\|u^s\|_{L^\infty(\Omega_+)} \leq \|S_k\|_{L^2(\Gamma) \rightarrow L^\infty(\Omega_+)} \|A_k^{-1}\|_{L^2(\Gamma) \rightarrow L^2(\Gamma)} \|f_k\|_{L^2(\Gamma)} \tag{1.4}$$

(ii) In rapports of the Dirichlet to Neumann map, we may ponder the BVP with Dirichlet data  $u^s = -u^{inc}$  on the boundary  $\partial\Omega$ , hence  $\partial_n^+ u^s = -P_{DtN} \tau_+ u^{inc}$ . We consequently have the illustration

$$u^s = -S_k (\partial_n^+ - P_{DtN} \tau_+) u^{inc}, \quad \text{in } \Omega_+,$$

which we can bound

$$\|u^s\|_{L^\infty(\Omega_+)} \leq \|S_k\|_{L^2(\partial\Omega) \rightarrow L^\infty(\Omega_+)} \left( 1 + \|P_{DtN}\|_{H_k^1(\partial\Omega) \rightarrow L^2(\partial\Omega)} \right) \|u^{inc}\|_{H_k^1(\partial\Omega)}$$

We have that  $\|S_k\|_{L^2(\partial\Omega) \rightarrow L^\infty(\Omega_+)} \leq k^{-1/2} \log^{1/2} k$  from [35, Lemma 4.1] provided we choose  $k_0 \geq \max\{2L_*, 2/L_*\}$ , also  $k_0$  must be chosen such that this proves the assertion. In the overhead Theorem 1.1, the bound (i) is a special case of the more general bound (ii), choosing  $k_0 = \max\{2L_*, 2/L_*\}$  and  $k$ -independent constant  $c = C_1 [2\text{diam}(\Omega_-) + 2]$ . In this chapter, we consider only convex polygons (a sub-class of star-shaped polygons, so all results concerning star-shaped obstacles hold), however Theorem 1.1(ii) is a general result which will also apply to multiple obstacles in non-convex obstacles.

### III. HERGLOTZ-TYPE PREVALENCE

First, we extend the well-studied case of plane wave occurrence to a weighted vital of plane waves. From the point of view of the mathematical analysis, this is the simplest case we consider, as flatness possessions are inherited from the single plane wave case. We aim to solve the problem for a single convex polygon  $\Omega_-$  with boundary  $\Gamma = \partial\Omega$ , where the occurrence field is a Herglotz-type function (in the sense of Definition 1.8), for which the Herglotz kernel  $g_{\text{Herg}} \in L^2(0, 2\pi)$  is known, henceforth

$$u^{\text{inc}}(\mathbf{x}) = u_{\text{Herg}}^{\text{inc}}(\mathbf{x}; g_{\text{Herg}}) := \int_0^{2\pi} g_{\text{Herg}}(\theta) e^{ik\mathbf{x} \cdot \mathbf{d}_\theta} d\theta, \quad \text{for } \mathbf{x} \in \mathbb{R}^2,$$

where  $\mathbf{d}_\theta := (\cos\theta, -\sin\theta)$ . We shall typically not stipulate the second argument (the Herglotz kernel) of  $u_{\text{Herg}}^{\text{inc}}(\mathbf{x}; g_{\text{Herg}})$ , and instead write  $u^{\text{inc}}_{\text{Herg}}(\mathbf{x})$ . We now separate the leading order behaviour (reflected terms) of  $\partial_{\mathbf{n}}^+ u$ , by piercing the incident wave  $u^{\text{inc}}_{\text{Herg}}$  into incoming and outgoing waves relative to the half-plane  $U_j$ ,

to obtain a representation of the form (1.2). To do this, we require  $Z_j^\downarrow := \{\theta \in [0, 2\pi) : \mathbf{d}_\theta \cdot \mathbf{n}_j < 0\}$  and  $Z_j^\uparrow := \{\theta \in [0, 2\pi) : \mathbf{d}_\theta \cdot \mathbf{n}_j \geq 0\}$ .

We may now split the incident wave into plane waves divided over these sets, and use the illustration (1.1) on  $Z_j^\uparrow$  to obtain for  $\mathbf{x}$  in  $U_j$

$$u_{\text{Herg}}^{\text{inc}}(\mathbf{x}) = \int_{Z_j^\downarrow \cup Z_j^\uparrow} g_{\text{Herg}}(\theta) e^{ik\mathbf{x} \cdot \mathbf{d}_\theta} d\theta$$

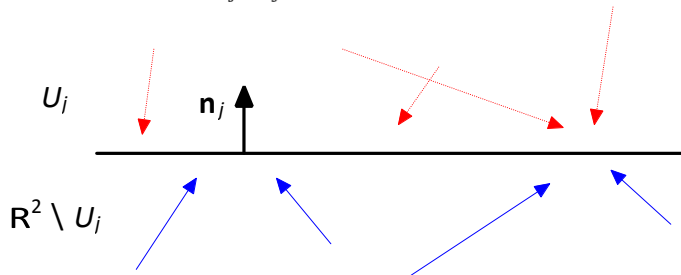


Figure 1.3: Example of the two types of waves split over the vital. Dashed arrows are those in  $Z_j^\downarrow$ , regular arrows are in  $Z_j^\uparrow$ .

$$= \int_{Z_j^\downarrow} g_{\text{Herg}}(\theta) e^{ik\mathbf{x} \cdot \mathbf{d}_\theta} d\theta + 2 \int_{\Gamma_j^\infty} \int_{Z_j^\uparrow} \frac{\partial \Phi(\mathbf{x}, \mathbf{y})}{\partial \mathbf{n}(\mathbf{y})} g_{\text{Herg}}(\theta) e^{ik\mathbf{y} \cdot \mathbf{d}_\theta} d\theta ds(\mathbf{y})$$

(1.5) We cannot use the representation (1.1) over  $Z_j^\downarrow$ , instead we may consider

$$u^r(\mathbf{x}) = -Z \int g_{\text{Herg}}(\theta) e^{ik\tilde{\mathbf{x}} \cdot \mathbf{d}_\theta} d\theta, \quad \mathbf{x} \text{ in } U_j, Z_j$$

the integral of images of plane waves reflected in the line  $\Gamma_j^\infty$  (see Figure 1.3). As this consists only of incident waves which are outgoing relative to  $\tilde{\mathbf{x}}_j$ , we can use the representation (1.1) with  $v = u^s$  to obtain

$$0 = u^r(\mathbf{x}) + 2 \int_{\Gamma_j^\infty} \int_{Z_j^\downarrow} \frac{\partial \Phi(\mathbf{x}, \mathbf{y})}{\partial \mathbf{n}(\mathbf{x})} g_{\text{Herg}}(\theta) e^{ik\mathbf{y} \cdot \mathbf{d}_\theta} d\theta ds(\mathbf{y}), \quad \mathbf{x} \text{ in } U_j, \quad (1.6)$$

where  $\tilde{\mathbf{y}}_j$  has been replaced by  $\mathbf{y}_j$ , as  $\mathbf{y} = \tilde{\mathbf{y}}_j$  on  $\Gamma_j^\infty$ . Summing (1.5), (1.6) and (1.1) with  $v = u^s$  yields

$$u(\mathbf{x}) = \int_{Z_j^\downarrow} g_{\text{Herg}}(\theta) [e^{ik\mathbf{x} \cdot \mathbf{d}_\theta} - e^{ik\tilde{\mathbf{x}} \cdot \mathbf{d}_\theta}] d\theta + 2 \int_{\Gamma_j^\infty} \frac{\partial \Phi(\mathbf{x}, \mathbf{y})}{\partial \mathbf{n}(\mathbf{y})} u(\mathbf{y}) ds(\mathbf{y}), \quad \mathbf{x} \text{ in } U_j, \quad (1.7)$$

finally taking the Neumann trace gives the representation (1.2)

$$\frac{\partial u}{\partial \mathbf{n}}(\mathbf{x}) = \Psi_{\text{Herg}}(\mathbf{x}) + 2 \int_{\Gamma_j^+ \cup \Gamma_j^-} \frac{\partial^2 \Phi(\mathbf{x}, \mathbf{y})}{\partial \mathbf{n}(\mathbf{x}) \partial \mathbf{n}(\mathbf{y})} u(\mathbf{y}) ds(\mathbf{y}), \quad \partial \mathbf{x} \text{ in } \Gamma_j, \quad (1.8)$$

where

$$\Psi_{\text{Herg}}(\mathbf{x}) = 2ik Z \int [\mathbf{n}_j \cdot \mathbf{d}_\theta] g_{\text{Herg}}(\theta) e^{ik\mathbf{x} \cdot \mathbf{d}_\theta} d\theta, \quad \mathbf{x} \text{ in } \Gamma_j, Z_j$$

We note that the representation (1.8) appears identical to (1.2), the key difference being the definition of  $\Psi = \Psi_{\text{Herg}}$ .

**THEOREM 1.2.** Suppose that the incident field is a Herglotz-type function  $u_{\text{Herg}}^{\text{inc}}$  (in the sense of Definition 1.8), and  $\Omega$  is a convex polygon. It follows that Assumption holds, with

$$M(u) = M_\infty(u) := \sup |u(\mathbf{x})|, \quad \mathbf{x} \in \Omega^+$$

hence the functions  $v_j^\pm, j = 1, \dots, n_\Gamma$ , are analytic in the right half-plane  $\text{Re}[s] > 0$ , where they satisfy the bounds

$$|v_j^\pm(s)| \leq \begin{cases} C_j^\pm M_\infty(u)k|ks|^{-\delta_j^\pm}, & 0 < |s| \leq 1/k, \\ C_j^\pm M_\infty(u)k|ks|^{-1/2}, & |s| > 1/k, \end{cases}$$

where  $\delta_j^+, \delta_j^- \in (0, 1/2)$  are given by  $\delta_j^+ := 1 - \pi/\omega_j$  and  $\delta_j^- := 1 - \pi/\omega_{j+1}$ . The constant  $C_j^+$  depends only on  $c_*$ , and  $\omega_j$ , whilst the constant  $C_j^-$  depends only on  $c_*$ , and  $\omega_{j+1}$ . Here the constants  $c_* \omega_j$  are as in Definition 2.1.

*Proof.* Given the boundary representation (1.8), [35, Theorem 1.1] describing the behaviour close to the corners holds for Herglotz-type functions, and the assertion follows by exactly the same arguments as [35, Theorem 1.2].  $\square$

The estimates above can be rewritten in terms of known parameters using the following bound.

**COROLLARY 1.1.** *Suppose that  $u^{\text{inc}}_{\text{Herg}}$  and  $\Omega_-$  are as in Theorem 1.2. Given the Herglotz kernel  $g_{\text{Herg}} \in L^2(0, 2\pi)$  of  $u^{\text{inc}}_{\text{Herg}}$  we have the following bound*

$$M_\infty(u) \leq \|g_{\text{Herg}}\|_{L^2(0, 2\pi)} \left( \sqrt{2\pi} + 2C_1 \sqrt{\pi} |\Gamma|^{1/2} \left[ \frac{1}{2\text{diam}(\Omega_-)} + \frac{1}{2k} \right] k^{1/2} \log^{1/2}(2 + kL_*) \right),$$

where  $C_1$  and  $L_*$  are as in Theorem 1.1. Hence, if there exists a  $\beta' > 0$  such that  $kg_{\text{Herg}}kL_2(0, 2\pi) \cdot k^{\beta'}$ , Assumption holds.

*Proof.* The bound on  $M_x(u)$  follows by writing

$$M_\infty(u) \leq \|u^{\text{inc}}_{\text{Herg}}\|_{L^\infty(\Omega_+)} + \|u^s\|_{L^\infty(\Omega_+)} \tag{1.9}$$

and noting by it follows that  $\|u^{\text{inc}}_{\text{Herg}}\|_{H^1_k(\Gamma)} \leq 2\sqrt{\pi} |\Gamma|^{1/2} k \|g_{\text{Herg}}\|_{L^2(0, 2\pi)}$ , hence we may use Theorem 1.1 to bound  $\|u^{\text{inc}}_{\text{Herg}}\|_{L^\infty(\Omega_+)}$  of (1.9), with  $\|u^{\text{inc}}_{\text{Herg}}\|_{L^\infty(\Omega_+)} \leq \sqrt{2\pi} kg_{\text{Herg}}kL_2(0, 2\pi)$ , which again follows.

Through Theorem 1.2 and Corollary (1.3), we have shown that both components of Assumption hold, exponential convergence of the Galerkin method for Herglotz-type incidence is guaranteed. We do not present numerical experiments for problems of Herglotz-type incidence here. Although the theory was initially developed to integrate HNA methods with the T-matrix method of [1], we will develop a more efficient method in which serves the same purpose, using the theory developed in [2]. To implement the theory of this section, one may apply the method to approximate  $\partial_n^+ u$ , noting that if we choose  $A = Ak$  then fully explicit error estimates follow from [3] on any  $N$ -dimensional subspace  $V_N^{\text{HNA}}(\Gamma)$ , by Corollary 1.1.

#### IV. SOURCE-TYPE PREVALENCE

In this section, we tend to aim to generalise the HNA technique to cases that the incident field  $u^{\text{inc}} \in C^\infty(\mathbb{R}^2)$ . Naturally, some regularity is needed for the HNA technique to figure. we tend to aim to contain the less regular regions of the incident field, for instance a degree at that the incident field is boundless, within a group that's sufficiently faraway from the scatterer  $\Omega_-$  specified Assumption holds, and so the HNA technique still converges at associate degree exponential rate. we tend to denote by  $Z$  a group within that this less regular behaviour is contained. Previous analyses of the HNA technique utilized the finitude of  $u$  once bounding the diffracted waves it follows from (1.2) that  $v_\pm$  may be written as integrals along the extended line  $\Gamma_j^\pm$ . The idea is to take  $M_x(u)$  outside of the integral using Hölder's inequality with  $L^1(\Gamma_j^\pm)$  and  $L^\infty(\Gamma_j^\pm)$ . However, we'll demonstrate here that if there exists a delimited open  $Z \in \mathbb{R}^2$  outside of that  $u^{\text{inc}}$  is sleek, it's sufficient on for  $u^{\text{inc}}$  to be  $L^2$  integrable on  $\Gamma_j^\pm \cap Z$ , while Theorem 1.1 provides a sure on  $ku^{\text{inc}}k_{\Gamma_j^\pm}$ . To ensure  $u^{\text{inc}}$  satisfies these conditions, we tend to outline the line

$$\ell_{c, \theta} := \{(x_1, x_2) \in \mathbb{R}^2 : x_2 \cos \theta - x_1 \sin \theta = c\}, \quad \text{for } c \in \mathbb{R} \text{ and } \theta \in [0, \pi). \tag{1.10}$$

We will make use of the following norm, which considers the trace on the intersection of such lines with  $Z$ , for a function  $w$

$$\|w\|_{\mathcal{L}(Z)} : H^{1/2+\epsilon}(Z) \rightarrow \mathbb{R}_+, \quad \|w\|_{\mathcal{L}(Z)} := \sup_{c \in \mathbb{R}, \theta \in [0, \pi)} \|\tau_{\ell_{c, \theta}} w\|_{L^2(\ell_{c, \theta} \cap Z)}, \quad \text{for } \varrho > 0, \tag{1.11}$$

where  $\tau_{\ell_{c, \theta}}$  denotes the trace operator mapping to the line  $\ell_{c, \theta}$ . Given that  $w \in H^{1/2+\varrho}(Z)$  we know that  $w$  is continuous across  $\ell_{c, \theta}$ , hence the trace is the same regardless of the direction in which it is taken. Figure 1.4 depicts the type of lines considered, for a set  $Z$ .

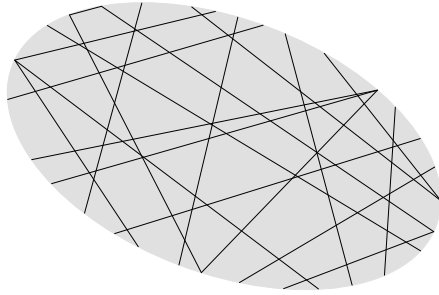


Figure 1.4: A finite set of lines intersecting some shaded region  $Z$ . The  $L(Z)$  norm considers the infinite set of all such lines, and bounds above the  $L^2$  norm of a function restricted to any such straight line.

The following Theorem bounds the  $L^2(\ell_{c,\theta} \cap Z)$  norm uniformly for any  $c \in \mathbb{R}, \theta \in [0, \pi)$ . This is useful given that our definition of  $M(u)$  for source-type incidence will contain the  $L(Z)$  norm.

**THEOREM 1.4.** *If  $u^{inc}|_Z \in H^s(Z)$  for  $s \in (1/2, 3/2)$ , where  $Z$  is a finite union of convex bounded sets open in  $\mathbb{R}^2$ , then*

$\|u^{inc}|_Z\|_{L^2(\partial Z)} \leq C_\tau \|u^{inc}|_Z\|_{H^s(Z)}$ , where  $C_\tau > 0$  depends only on  $Z$ . *Proof.* Initially we consider the case for  $Z$  convex. We consider a line  $\ell_{c,\theta}$  which intersects  $Z$ , and consider the two (also convex) sets formed via the bisection of the set  $Z$  by  $\ell_{c,\theta}$ . Denote by one of these two sets  $Z^*$ , chosen to be the set inside of which the largest ball can be constructed, and assume for now that  $\text{diam}(Z^*) = 1$ . Denote by  $\partial Z^*$  the boundary of  $Z^*$ . It follows by [36, Lemma 4.4] that

$$\|w\|_{L^2(\partial Z^*)}^2 \leq \hat{C}_\tau \left( \|w\|_{L^2(Z^*)}^2 + |w|_{W^s(Z^*)}^2 \right), \quad \text{for } w \in H^s(Z^*),$$

where  $\hat{C}_\tau$  depends on  $Z^*$  and  $|\cdot|_{W^s(Z^*)}$  denotes the Sobolev–Slobodeckij semi-norm, order  $s$  over  $Z^*$  (see e.g. [42, p74] for a definition). As  $\ell_{c,\theta} \cap Z \subset \partial Z^*$ , and  $Z^* \subset Z$  we have

$$\|w\|_{L^2(\ell_{c,\theta} \cap Z)}^2 \leq \hat{C}_\tau \left( \|w\|_{L^2(Z)}^2 + |w|_{W^s(Z)}^2 \right), \quad \text{for } w \in H^s(Z).$$

Given the conditions of [36, Lemma 4.4], we may choose  $\hat{C}_\tau$  to be the constant corresponding to the  $\ell_{c,\theta}$  which minimises the radius of the largest open ball that can be constructed inside of the set  $Z^*$ . Given  $Z$ , this choice will produce the maximal value of  $\hat{C}_\tau$ . Combining this maximal constant with the equivalence of the Sobolev–Slobodeckij and Bessel potential norms (see, Theorem 1.30(ii)) we may write  $\|w\|_{L^2(\ell_{c,\theta} \cap Z)} \leq C_\tau \|w\|_{H^s(Z)}$ , for  $w \in H^s(Z)$ , where  $C_\tau$  depends only on  $Z$ . Repeated applications of the above steps extend this result to finite unions of convex sets. Likewise, scaling arguments can be used for the case  $\text{diam}(Z^*) = 1.6$  Now we may define the space of source-type incident waves which we will solve via the HNA method.

**DEFINITION 1.5** (Source-type incidence). *Given a bounded open  $Z \subset \mathbb{R}^2$  such that  $\text{dist}(Z, \Omega_+) \geq 1/k$ , we define the set of source-type incidences as*

$$H_{\text{src}}(\Omega_+; Z) := \{ \varphi \in L^2_{\text{loc}}(\mathbb{R}^2) : \varphi|_Z \in H^s(Z), \text{ for } s > 1/2, \quad \phi|_{\mathbb{R}^2 \setminus Z} \in C^\infty(\mathbb{R}^2 \setminus Z) \}.$$

The above definition takes into consideration the result of Theorem 1.4; by restricting to  $\phi|_Z \in H^s(Z)$  this ensures that  $\| \phi \|_{L^2(Z)} < \infty$  for all functions in the space. We note also that classical  $C^\infty(\mathbb{R}^2)$  incidences, for example plane or Herglotz-type waves, are accommodated by the above definition, in which case  $Z$  may be chosen to be empty.

Intuitively, the set  $Z$  can be thought of as the region in which the incident wave may be less regular, and all weakly singular behaviour should be strictly inside of  $Z$ . Given that we still have smoothness inside a neighbourhood of  $\Gamma$ , we can obtain the required bounds on  $|v_\pm|$  for a carefully chosen  $M(u)$ .

## V. FOREMOST DIRECTIVE BEHAVIOUR FOR SCATTERING BY POINT AND BEAM SOURCE PREVALENCE

We currently limit our attention to a selected category of source-type incident fields, in order that the leading order behaviour is separated, as is needed to represent the answer within the type (1.2)

**DEFINITION 1.6** (Localised source). *The localised source  $u^{inc} \in H_{\text{src}}(\Omega_+, Z)$  is defined as  $u^{inc}(\mathbf{x}) = \langle \phi, \tilde{\Phi}(\mathbf{x}, \cdot) \rangle$ , for  $\mathbf{x} \in \mathbb{R}^2 \setminus Z$ ,*

*where  $\tilde{\phi}$  is a distribution, and the values of  $Z$  for which  $\mathbf{x}$  is defined depends on the particular choice of  $\tilde{\phi}$ , as discussed in Remark 1.7 below. We are interested in two particular cases:*

- (i) The point source emanating from  $\mathbf{s} \in Z$ , corresponding to  $\tilde{\phi} = \delta_{\mathbf{s}}$ , where  $\delta_{\mathbf{s}}$  is the Dirac Delta function translated to  $\mathbf{s}$ , for which

$$u^{inc}(\mathbf{x}) = u^{inc}_{PS}(\mathbf{x};\mathbf{s}) := \Phi(\mathbf{x},\mathbf{s}), \quad \text{for } \mathbf{x} \in \mathbb{R}^2 \setminus \{\mathbf{s}\}.$$

- (ii) The beam source emanating from a Lipschitz curve  $\gamma$  of Hausdorff dimension one, with density  $\phi \in L^2(\gamma)$ ,

$$u^{inc}(\mathbf{x}) = u^{inc}_{BS}(\mathbf{x};\phi) := \int_Z \Phi(\mathbf{x},\mathbf{y})\phi(\mathbf{y})d\mathbf{s}(\mathbf{y}), \quad \text{for } \mathbf{x} \in \mathbb{R}^2 \setminus \gamma$$

See Figure 1.6 for examples of typical  $Z$  for source type waves. Hereafter we shall often make the second arguments  $\mathbf{s}$  and  $\phi$  of  $u^{inc}_{PS}$  and  $u^{inc}_{BS}$  implicit, writing  $u^{inc}_{PS}(\mathbf{x})$  and  $u^{inc}_{BS}(\mathbf{x})$  instead.

**REMARK 1.7** (Dependence on regularity of  $\tilde{\phi}$ ). We now explain in more detail the values of  $\mathbf{x} \in Z$  for which  $u^{inc}(\mathbf{x})$  is defined, given  $\tilde{\phi}$ , noting the regularity of the fundamental solution,

$$\Phi(\mathbf{x}, \cdot) \in H^{1-\varrho}(\mathbb{R}^2), \quad \text{for all } \varrho > 0, \quad \text{for all } \mathbf{x} \in \mathbb{R}^2. \quad (1.12)$$

(As we could not locate a derivation of the regularity (1.12) in the literature, we present an argument in Appendix A.4.) Given that the inner product is well defined between any space and its dual, it follows from (1.12) that  $u^{inc}(\mathbf{x}) = \langle \tilde{\phi}, \Phi(\mathbf{x}, \cdot) \rangle$  is defined for all  $\mathbf{x} \in Z$  (and therefore all  $\mathbf{x} \in \mathbb{R}^2$ ) if  $\tilde{\phi} \in H^{-1+\varrho}(\mathbb{R}^2)$ , as is the case for the beam source of Definition 1.6(ii). However, this is not the case for the point source, as we have taken the less regular  $\tilde{\phi} = \delta_{\mathbf{s}} \in H^{-1+\varrho}(Z) \cap (C(Z))^*$ , for  $\mathbf{s} \in Z$  and  $\varrho > 0$ , yielding  $\Phi(\mathbf{x},\mathbf{s})$ , for which  $\mathbf{x}$  is undefined at  $\mathbf{s}$ . However, for the point source case, it follows from (1.12) that  $\Phi(\cdot, \mathbf{s}) \in H^{\varrho}(\mathbb{R}^2)$  for  $s \in (1/2, 1)$ , hence by Definition 1.5 we have that  $\Phi(\cdot, \mathbf{s}) \in H_{src}(\Omega_+; Z)$  for  $\mathbf{s}$  in a suitable  $Z$  containing  $\mathbf{s}$ . This is sufficient to prove the bounds on  $|v_{\pm}|$ , as required. Now we derive a representation for  $\partial_{\mathbf{n}}^+ u$  which explicitly separates the leading order (reflected) terms in terms of known components of  $u^{inc}$ , for the case of the beam source and the point source. The general rule is that if the side  $\Gamma_j$  can see the source, then the leading order term  $\Psi$  is equal to  $2\partial_{\mathbf{n}}^+ u^{inc}$ , otherwise it is equal to zero.

**THEOREM 1.8.** For a point source incidence  $u^{inc} = u^{inc}_{PS}$  (as in Definition 1.6(i)), the leading order behaviour of

$$\Psi = \Psi_{PS}(\mathbf{x}) := \begin{cases} (1.2) \text{ is} \\ \mathbf{n} \cdot 2\partial^+ \Phi(\mathbf{x},\mathbf{s}), & \mathbf{s} \in U_j, \\ 0, & \text{otherwise,} \end{cases} \quad \text{for } \mathbf{x} \in \Gamma_j, \quad (1.13)$$

where  $U_j$  denotes the upper half plane relative to  $\Gamma_j^{\infty}$  (as defined at the start of this Chapter, depicted in Figure 1.1).

*Proof.* Define the half-plane Dirichlet Green's function

$$G_j(\mathbf{x}, \mathbf{y}) := \Phi(\mathbf{x}, \mathbf{y}) - \Phi(\mathbf{x}^j, \mathbf{y}), \quad \mathbf{x} = \mathbf{y},$$

where  $\mathbf{x}^j$  is the reflection of  $\mathbf{x}$  in the line  $\Gamma_j^{\infty}$ , as defined at the beginning of this chapter. We split into three cases, depending on the position of the source point:

- (i) For  $\mathbf{s} \in U_j$ , we apply Green's second identity to  $u^{inc}_{PS}$  and  $G_j(\mathbf{x}, \cdot)$  in  $U_j \cap B_R(0) \cap B_{\varrho}(\mathbf{s})$ , where  $B_R$  is a ball chosen sufficiently large that  $\Gamma_j$  and  $B_{\varrho}(\mathbf{s})$  are inside it, for  $\varrho > 0$ . Taking the limit as  $\varrho \rightarrow 0$  and  $R \rightarrow \infty$  yields the result

$$u^{inc}_{PS}(\mathbf{x}) = G_j(\mathbf{x}, \mathbf{s}) + 2 \int_{\Gamma_j^{\infty}} \frac{\partial \Phi(\mathbf{x}, \mathbf{y})}{\partial \mathbf{n}(\mathbf{y})} u^{inc}_{PS}(\mathbf{y}) d\mathbf{s}(\mathbf{y}), \quad \mathbf{x} \in U_j. \quad (1.14)$$

Taking the Neumann trace gives the result

$$\frac{\partial u^{inc}_{PS}}{\partial \mathbf{n}}(\mathbf{x}) = 2 \frac{\partial \Phi(\mathbf{x}, \mathbf{s})}{\partial \mathbf{n}(\mathbf{x})} + 2 \int_{\Gamma_j^{\infty}} \frac{\partial^2 \Phi(\mathbf{x}, \mathbf{y})}{\partial \mathbf{n}(\mathbf{x}) \partial \mathbf{n}(\mathbf{y})} u^{inc}_{PS}(\mathbf{y}) d\mathbf{s}(\mathbf{y}), \quad \mathbf{x} \in \Gamma_j, \quad (1.15)$$

as claimed.

- (ii) For  $\mathbf{s} \in \Gamma_j^{\infty}$ , the same approach as (i) holds, although the factor of 2 in (1.14) is replaced by a 1, as only half of the  $\varrho$ -ball is in  $U_j$ . This makes no difference however, as  $\partial_{\mathbf{n}}^+ \Phi(\mathbf{x}, \mathbf{s}) = 0$  for  $\mathbf{s} \in \Gamma_j^{\infty}$ , so the leading order term  $\Psi$  is zero in this case.
- (iii) For a source in the relative lower-half plane,  $\mathbf{s} \in \mathbb{R}^2 \setminus U_j$ , the representation (1.1) may be used, as  $u^{inc}_{PS}$  is smooth in the upper half plane  $U_j$ , hence

$$u^{inc}_{PS}(\mathbf{x}) = 2 \int_{\Gamma_j^{\infty}} \frac{\partial \Phi(\mathbf{x}, \mathbf{y})}{\partial \mathbf{n}(\mathbf{y})} u^{inc}_{PS}(\mathbf{y}) d\mathbf{s}(\mathbf{y}), \quad \mathbf{x} \in U_j,$$

and taking the Neumann trace yields

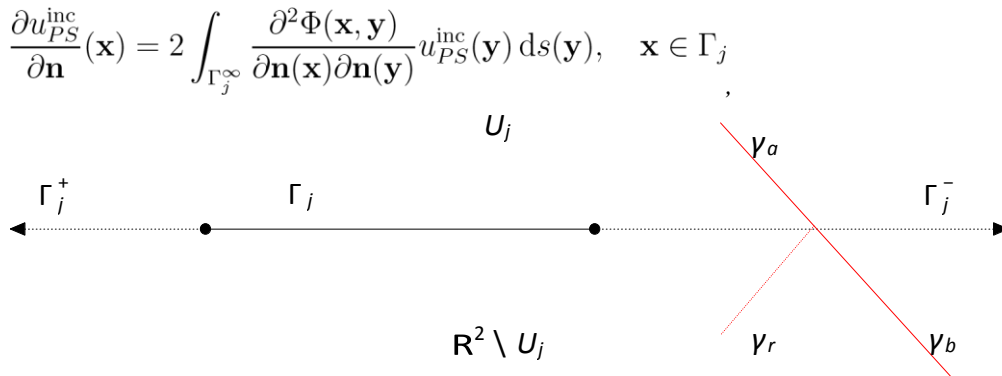


Figure 1.5: Depiction of the imaging argument used in the proof of Theorem 1.9. Here  $\gamma_a := \gamma \cap U_j$ ,  $\gamma_b := \gamma \setminus U_j$  and  $\gamma_r := \{\tilde{\mathbf{x}}_j \in \mathbb{R}^2 : \mathbf{x} \in \gamma_a\}$ . Physically,  $\gamma_r$  corresponds to the reflection of  $\gamma_a$  in the line  $\gamma_j^\infty := \Gamma_j^- \cup \Gamma_j \cup \Gamma_j^+$ . The wave  $u_a^{\text{inc}}$  emanates from  $\gamma_a$ ,  $u_b^{\text{inc}}$  emanates from  $\gamma_b$ , and  $u_a^r$  may be interpreted as a wave emanating from  $\gamma_r$  (although it is formulated differently in (1.20)).

Combining each case, summing with the representation (1.19) of the Neumann trace of the scattered field  $u^s$  yields

$$\frac{\partial u}{\partial \mathbf{n}}(\mathbf{x}) = \Psi_{\text{PS}}(\mathbf{x}) + 2 \int_{\Gamma_j^+ \cup \Gamma_j^-} \frac{\partial \Phi(\mathbf{x}, \mathbf{y})}{\partial \mathbf{n}(\mathbf{x}) \partial \mathbf{n}(\mathbf{y})} u(\mathbf{y}) \, ds(\mathbf{y}), \quad \mathbf{x} \in \Gamma_j,$$

as claimed  $\square$

**THEOREM 1.9.** For a beam source incidence  $u^{\text{inc}} = u^{\text{inc}}_{\text{BS}}$  with density  $\phi \in L^2(\gamma)$  (as in Definition 1.6(ii)), the leading order behaviour of (1.2) is

$$\Psi_{\text{BS}}(\mathbf{x}) = 2 \int_{U_j \cap \gamma} \frac{\partial \Phi(\mathbf{x}, \mathbf{y})}{\partial \mathbf{n}(\mathbf{x})} \phi(\mathbf{y}) \, ds(\mathbf{y}), \quad \text{for } \mathbf{x} \in \Gamma_j. \tag{1.16}$$

*Proof.* We will use a *method of images* style argument (depicted in Figure 1.5). We split  $u^{\text{inc}}_{\text{BS}}$  into two components, corresponding to the contribution to the intensity at  $\mathbf{x}$  from the components of the incident field above and below the extended line  $\Gamma_j^\infty$ ,  $u_a^{\text{inc}}(\mathbf{x}) := \int_{U_j \cap \gamma} \Phi(\mathbf{x}, \mathbf{y}) \phi(\mathbf{y}) \, ds(\mathbf{y})$ , and  $u_b^{\text{inc}}(\mathbf{x}) := \int_{\gamma \cap U_j \setminus U_j} \Phi(\mathbf{x}, \mathbf{y}) \phi(\mathbf{y}) \, ds(\mathbf{y})$ , (1.17)

noting that  $u^{\text{inc}} = u_a^{\text{inc}} + u_b^{\text{inc}}$ . Given that  $u_b^{\text{inc}}|_{U_j} \in C^2(U_j) \cap C(U_j)$ , we can apply (1.1) to obtain the representation

$$u_b^{\text{inc}}(\mathbf{x}) = \int_{\Gamma_j^\infty} \frac{\partial \Phi(\mathbf{x}, \mathbf{y})}{\partial \mathbf{n}(\mathbf{y})} u_b^{\text{inc}}(\mathbf{y}) \, ds(\mathbf{y}), \quad \mathbf{x} \in U_j. \tag{1.18}$$

We note that the same representation holds for  $u^s$ , hence

$$u^s(\mathbf{x}) = \int_{\Gamma_j^\infty} \frac{\partial \Phi(\mathbf{x}, \mathbf{y})}{\partial \mathbf{n}(\mathbf{y})} u^s(\mathbf{y}) \, ds(\mathbf{y}), \quad \mathbf{x} \in U_j. \tag{1.19}$$

For  $\phi \in L^2(\gamma)$ , it follows from [13, Theorem 2.15] that  $u_a^{\text{inc}}|_{U_j} \in H_{\text{loc}}^{3/2}(U_j) \not\subset C^2(U_j) \cap C(U_j)$ , hence we cannot apply (1.1). Instead we make use of  $u_a^r(\mathbf{x}) := -u_a^{\text{inc}}(\tilde{\mathbf{x}}_j) \in C^2(U_j) \cap C(\overline{U_j})$ , which physically corresponds to the reflection of  $u_a^{\text{inc}}$  in the extended line  $\Gamma_j^\infty$  (See Figure 1.5). Applying (1.1) yields

$$u_a^r(\mathbf{x}) = 2 \int_{\Gamma_j^\infty} \frac{\partial \Phi(\tilde{\mathbf{x}}_j, \mathbf{y})}{\partial \mathbf{n}(\mathbf{y})} u_a^{\text{inc}}(\mathbf{y}) \, ds(\mathbf{y}) = -2 \int_{\Gamma_j^\infty} \frac{\partial \Phi(\mathbf{x}, \mathbf{y})}{\partial \mathbf{n}(\mathbf{y})} u_a^{\text{inc}}(\mathbf{y}) \, ds(\mathbf{y}), \tag{3.20}$$

for  $\mathbf{x} \in U_j$ . We may now add both sides of (1.20) to  $u = u^{\text{inc}} + u^s$ , and split the incident field  $u^{\text{inc}} = u_a^{\text{inc}} + u_b^{\text{inc}}$  to obtain

$$u(\mathbf{x}) = \underbrace{u_a^{\text{inc}}(\mathbf{x}) + u_b^{\text{inc}}(\mathbf{x})}_{u^{\text{inc}}} + u^s(\mathbf{x}) + u_a^r(\mathbf{x}) + 2 \int_{\Gamma_j^\infty} \frac{\partial \Phi(\mathbf{x}, \mathbf{y})}{\partial \mathbf{n}(\mathbf{y})} u_a^{\text{inc}}(\mathbf{y}) \, ds(\mathbf{y}), \quad \mathbf{x} \in U_j,$$

Substituting the representation for  $u_a^{\text{inc}}$  of (1.17) and (1.19), we obtain

$$u(\mathbf{x}) = u_a^{inc}(\mathbf{x}) + u_a^r(\mathbf{x}) + 2 \int_{\Gamma_j^+ \cup \Gamma_j^-} \frac{\partial \Phi(\mathbf{x}, \mathbf{y})}{\partial \mathbf{n}(\mathbf{y})} u(\mathbf{y}) \, ds(\mathbf{y}), \quad \mathbf{x} \in U_j.$$

Taking the Neumann trace to  $\Gamma_j$  yields

$$\frac{\partial u}{\partial \mathbf{n}}(\mathbf{x}) = 2 \int_{\gamma \cap U_j} \frac{\partial \Phi(\mathbf{x}, \mathbf{y})}{\partial \mathbf{n}(\mathbf{x})} \varphi(\mathbf{y}) \, ds(\mathbf{y}) + 2 \int_{\Gamma_j^+ \cup \Gamma_j^-} \frac{\partial^2 \Phi(\mathbf{x}, \mathbf{y})}{\partial \mathbf{n}(\mathbf{x}) \partial \mathbf{n}(\mathbf{y})} u(\mathbf{y}) \, ds(\mathbf{y}), \quad \mathbf{x} \in \Gamma_j,$$

as claimed.

The definition of  $\Psi$  for purpose some extent degree supply is also simply extended to multiple point sources by taking a linear combination of the leading order by taking a linear combination of the leading order behaviour for every individual point source. Recalling that the beam supply could become a helpful construct in unvaried multiple scattering ways, we tend to remark that the case of a a lot of general density density  $\phi \in H^{-1/2}(\gamma)$  should be understood for associate unvaried resolution of a configuration of multiple screens, as this can be the answer area of the screen downside. we tend to speculate that an analogous result holds in such a case, but one should watch out once ripping the beam supply into  $u^{inc} = u_a^{inc} + u_b^{inc}$ , because the integral currently should be understood within the sense of distributions.

We will see that the leading order for beam supply incidence is closely associated with our multiple scattering operator; the key distinction is that  $\phi$  becomes associate unknown density within the multiple scattering case.

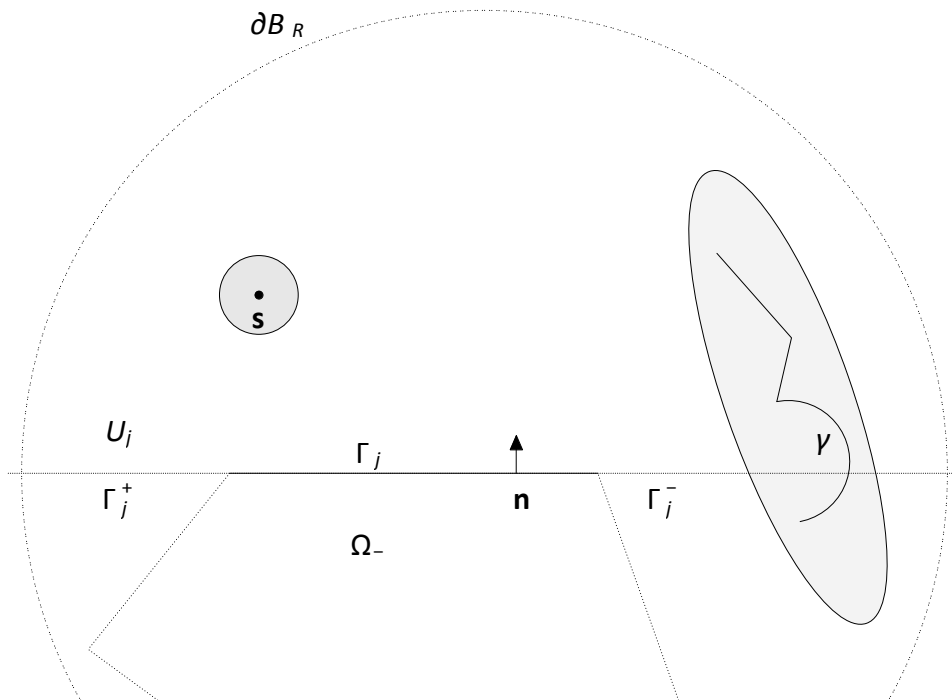


Figure 1.6: Example of components used for half-plane representation, in which the shaded region(s) denote(s) the choice of  $Z$ . This diagram may be used to explain the point source (at  $s$ ) or beam source (at  $\gamma$ ) case, or the incident wave corresponding to the combination of both.

## VI. REGULARITY OF $V_{\pm}$ FOR SOURCE-TYPE TERMS

In the previous subsection we separated the leading order behaviour for a large class of source-type incidences, of the form stated in Definition 1.6. We now relax further, to the entire space  $H_{src}(\Omega_+; Z)$ , inside of which we prove the required bounds on the diffracted waves.

**THEOREM 1.10.** For incident field  $u^{inc}$ , if there exists  $Z$  such that  $u^{inc} \in H_{src}(\Omega_+; Z)$  (as in Definition 1.5), then Assumption 2.4 holds with  $M(u) = M_Z(u)$ , that is

$$M_Z(u) := \|u^{inc}\|_{L^\infty(\Omega_+ \setminus Z)} + \|u^s\|_{L^\infty(\Omega_+)} + \sqrt{\frac{k}{8}} \|u^{inc}\|_{\mathcal{L}(Z)}. \quad (1.21)$$

Hence the functions  $v_j^\pm$ , for  $j = 1, \dots, n_\Gamma$ , are analytic in the right half-plane  $\text{Re}[s] > 0$ , where they satisfy the bounds

$$|v_j^\pm(s)| \leq \begin{cases} C_j^\pm M_Z(u)k|ks|^{-\delta_j^\pm}, & 0 < |s| \leq 1/k, \\ C_j^\pm M_Z(u)k|ks|^{-1/2}, & |s| > 1/k, \end{cases}$$

where  $\delta_j^+, \delta_j^- \in (0, 1/2)$  are given by  $\delta_j^+ := 1 - \pi/\omega_j$  and  $\delta_j^- := 1 - \pi/\omega_{j+1}$ . The constant  $C_j^+$  depends only on  $c_*$ , and  $\omega_j$ , whilst the constant  $C_j^-$  depends only on  $c_*$ , and  $\omega_{j+1}$ .

*Proof.* The analyticity of the functions  $v_j^\pm(s)$  in  $\text{Re}[s] > 0$  follows from the analyticity of  $\mu(s)$  in the same set, which is shown in [35, Lemma 1.4].

Firstly we deal with the case of  $|s| > 1/k$ . It follows that  $k(s+t) > 1$ , hence the bound [35, (1.7)] can be simplified and we may write

$$(1.22) \quad |v_j^+(s)| \leq \frac{k^2}{2} \int_0^\infty |\mu(k(s+t))|^{-3/2} \left| u\left(\mathbf{y}_j(\tilde{L}_{j-1} - t)\right) \right| dt$$

We now split the separating the integral, set  $Z' \subset (1/k, \infty)$

$$\leq \frac{k^2}{2} \int_0^\infty k(|s|+t)^{-3/2} \left| u\left(\mathbf{y}_j(\tilde{L}_{j-1} - t)\right) \right| dt.$$

containing all  $t$  such that  $\mathbf{y}_j(\tilde{L}_{j-1} - t) \in Z$ . It follows that

$$\begin{aligned} & \frac{k^2}{2} \int_{Z'} (k(|s|+t))^{-3/2} \left| u^{\text{inc}}\left(\mathbf{y}_j(\tilde{L}_{j-1} - t)\right) \right| \\ & /k \text{ and } Z' \text{ is bounded, we can write} \\ |v_j^+(s)| & \leq \frac{k^2}{2} \left[ \int_{(0,\infty)\setminus Z'} + \int_{Z'} \right] k(|s|+t)^{-3/2} \left| u\left(\mathbf{y}_j(\tilde{L}_{j-1} - t)\right) \right| dt, \\ & \leq \frac{k^2}{2} (\|u\|_{L^\infty(D\setminus Z)}) \int_{(0,\infty)\setminus Z'} k(|s|+t) dt \\ & \quad + \frac{k^2}{2} \int_{Z'} k(|s|+t)^{-3/2} \left| u\left(\mathbf{y}_j(\tilde{L}_{j-1} - t)\right) \right| dt \\ & \leq \frac{k^2}{2} (\|u\|_{L^\infty(D\setminus Z)}) \int_{(0,\infty)\setminus Z'} k(|s|+t) dt + \frac{k^2}{2} \|u^s\|_{L^\infty(Z)} \int_{Z'} k(|s|+t)^{-3/2} dt \end{aligned}$$

Since  $|s| > 1$

$$\int_0^\infty (k(|s|+t))^{-3/2} dt \leq 2k^{-1}|ks|^{-1/2}$$

and

$$\left( \int_{Z'} |k(|s|+t)|^{-3} dt \right)^{1/2} \leq \frac{k^{-1/2}}{\sqrt{2}} |ks|^{-1} \leq \frac{k^{-1/2}}{\sqrt{2}} |ks|^{-1/2},$$

hence by the Cauchy-Schwarz inequality

$$|v_j^+(s)| \leq M_Z(u)k|ks|^{-1/2} \quad \text{for } s > \frac{1}{k}.$$

For  $|s| \leq 1/k$ , the definition of  $v_j^+$  gives

$$|v_j^+(s)| \leq \frac{k^2}{2} \left[ \int_0^{1/k} + \int_{1/k}^\infty \right] |\mu(k(s+t))| \left| u\left(\mathbf{y}_j(\tilde{L}_{j-1} - t)\right) \right| dt$$

As  $(0, 1/k) \subset Z$ , it follows from the Definition of  $H_{\text{src}}(\Omega_+; Z)$  that  $u^{\text{inc}}$  is infinitely differentiable in this region, and satisfies [35, Lemma 1.5], hence

$$u(\mathbf{x}) \leq CkL^\infty(\Omega_+; Z)(k|\mathbf{x}|)^{\pi/\omega_j}, \text{ for } |\mathbf{x}| < 1/k, \text{ for } C \text{ independent of } k, \text{ and } u(\mathbf{x}) \leq CM_Z(u)(k|\mathbf{x}|)^{\pi/\omega_j}, \text{ for } |\mathbf{x}| < 1/k. \text{ The first integral is bounded as in the proof of [35, Theorem 1.2], hence}$$

$$\begin{aligned} \int_0^{1/k} |\mu(k(s+t))| |u(\mathbf{y}_j(\tilde{L}_{j-1}-t))| dt &\leq \|u(\mathbf{y}_j(\tilde{L}_{j-1}-t))\|_{L^\infty(0,1/k)} k |ks|^{-\delta_j^\pm} \\ &\leq k (\|u^{\text{inc}}\|_{L^\infty(\Omega_+ \setminus Z)} + \|u^s\|_{L^\infty(\Omega_+)}) |ks|^{-\delta_j^\pm} \\ &\leq k (\|u^{\text{inc}}\|_{L^\infty(\Omega_+ \setminus Z)} + \|u^s\|_{L^\infty(\Omega_+)}) |ks|^{-\delta_j^\pm}, \end{aligned} \tag{3.24}$$

whilst the second fundamental is bounded as in the case  $|s| > 1/k$ . Coalescing all bounds proves the declaration. Provided that  $M_Z(u)$  has only numerical growth in  $k$ , the conditions are satisfied, and a *hp* method as described converges exponentially. We note again that up to this point, the case  $u^{\text{inc}} \in C^\infty(\mathbb{R}^2)$  also fits inside of this framework, by choosing  $Z$  empty. We now seek fully unambiguous bounds on  $M_Z(u)$  for the case of point source incidence.

**THEOREM 1.11.** For point source incidence  $u^{\text{inc}} = u^{\text{inc}}_{PS}(\cdot; \mathbf{s})$  with  $\text{dist}(\mathbf{s}, \Gamma) > 1/k$ , it follows that  $u^{\text{inc}}_{PS} \in H_{\text{src}}(\Omega_+; Z)$  (of Definition 1.5) with  $Z = B_r(\mathbf{s})$  and  $r = \min(1, 1/(2k))$ , moreover we have a  $k$ -explicit bound on the constant of Theorem 1.10

$$M_Z(u) \leq C_2 + \frac{C_1 |\Gamma|^{1/2}}{2} \left[ \frac{1}{2 \text{diam}(\Omega_+)} + \frac{1}{k} \right] \log^{1/2}(2 + kL_*) \left( \sqrt{\frac{2}{\pi \text{dist}(\mathbf{s}, \Gamma)}} + \frac{1}{\pi \text{dist}(\mathbf{s}, \Gamma) \sqrt{k}} \right),$$

where  $C_1$  and  $L_*$  are the constants from Theorem 1.1, and

$$C_2 = \frac{1}{2\sqrt{\pi}} + \frac{1}{\sqrt{2}} \left( 1 + \frac{2}{\pi} (1 + \gamma_E + e^{1/4}) \right) (5 + \log^2 2 + \log 16)^{1/2}.$$

*Proof.* Noting the definition (1.21) of  $M_Z(u)$ , we bound each of the three components separately.

(i) The bound on

$$\|u^{\text{inc}}_{PS}\|_{L^\infty(\Omega_+ \setminus Z)} \leq \frac{1}{2\sqrt{\pi}}$$

follows immediately from (A.7); given the monotonicity of the absolute value of Hankel functions, the maximal value will occur at the boundary of  $Z$ .

(ii) Secondly we prove the bound on  $ku^s k L^\infty(\Omega_+)$ . By Definition A.4 of the  $H_k^1$  norm, we have

$$\|u^{\text{inc}}_{PS}\|_{H_k^1(\Gamma)} = \left( \int_\Gamma k^2 |\Phi(\mathbf{y}, \mathbf{s})|^2 + |\nabla_\Gamma \Phi(\mathbf{y}, \mathbf{s})|^2 ds(\mathbf{y}) \right)^{1/2},$$

which we can bound using  $(a+b)^{1/2} \leq a+b$  for  $a$  and  $b$  non-negative, hence

$$\|u^{\text{inc}}_{PS}\|_{H_k^1(\Gamma)} = |\Gamma|^{1/2} \left( \sup_{\mathbf{y} \in \Gamma} k^2 |\Phi(\mathbf{y}, \mathbf{s})|^2 + \sup_{\mathbf{y} \in \Gamma} |\nabla_\Gamma \Phi(\mathbf{y}, \mathbf{s})|^2 ds(\mathbf{y}) \right)^{1/2}.$$

Given the definition of  $\Phi$ , and that  $H_0^{(1)}(kz) = -kH_1^{(1)}(kz)$  for  $z > 0$ , using (A.7) and (A.8) to bound these yields

$$\|u^{\text{inc}}_{PS}\|_{H_k^1(\Gamma)} \leq \frac{|\Gamma|^{1/2}}{2} \left( \sqrt{\frac{2k}{\pi \text{dist}(\mathbf{s}, \Omega_+)}} + \frac{1}{\pi \text{dist}(\mathbf{s}, \Omega_+)} \right).$$

Combining with Theorem 1.1, we obtain

$$\begin{aligned} &\|u^s\|_{L^\infty(\Omega_+)} \\ &\leq \frac{C_1 |\Gamma|^{1/2}}{2} \left[ \frac{1}{2 \text{diam}(\Omega_+)} + \frac{1}{k} \right] \log^{1/2}(2 + kL_*) \left( \sqrt{\frac{2}{\pi \text{dist}(\mathbf{s}, \Gamma)}} + \frac{1}{\pi \text{dist}(\mathbf{s}, \Gamma) \sqrt{k}} \right), \end{aligned}$$

(iii) Thirdly we prove the bound on  $ku^{\text{inc}}_{PS} k L(Z)$ . We choose  $\ell_*$  to be a line of the form (1.10) containing  $\mathbf{s}$ ; given the monotonicity of  $|\Phi(\cdot, \mathbf{s})|$ , this line will maximise the norm. By definition of  $\Phi$  and the  $L^2$  norm,

Using (A.10) we can write  $\|u_{PS}^{inc}\|_{L^2(\ell_* \cap Z)}^2 = 2 \int_0^{\frac{1}{2k}} \left| \frac{1}{4} H_0^{(1)}(kt) \right|^2 dt$ .

$$\begin{aligned} \|u_{PS}^{inc}\|_{L^2(\ell_* \cap Z)}^2 &\leq \frac{1}{8} \int_0^{\frac{1}{2k}} \hat{c}^2 (1 + |\log(kt)|)^2 dt \\ &= \frac{1}{8k} \hat{c}^2 (5 + \log^2 2 + \log 16) \end{aligned}$$

hence

$$\|u_{PS}^{inc}\|_{L^2(\ell_* \cap Z)} \leq \frac{1}{2\sqrt{2k}} \hat{c} (5 + \log^2 2 + \log 16)^{1/2}$$

Noting the definition (1.21), it follows from (i) and (iii) that

$$C_2 = \|u_{PS}^{inc}\|_{L^\infty(\Omega_+ \setminus Z)} + \sqrt{\frac{k}{8}} \|u_{PS}^{inc}\|_{L^2(\ell_* \cap Z)}$$

the result follows, with (ii) contributing the  $k$ -dependent components of the bound.

Now we prove a similar result for the beam source case.

**THEOREM 1.12.** Suppose  $u^{inc}_{BS}$  is a beam source incidence (in the sense of Definition 1.6(ii)) with density  $\phi \in L^2(\gamma)$ , emanating from  $\gamma$  with  $\text{dist}(\gamma, \Omega_+) \geq 1/k$ . If  $M(u) = M_Z(u)$  where  $Z$  is a bounded open neighbourhood containing  $\gamma$ , or if  $M(u) = M_\infty(u)$ , then given  $k_0 > 0$  we have the bound

$$M(u) \cdot \log^{1/2}(k) k \phi k_{L^2(\gamma)}, \quad \text{for } k \geq k_0.$$

Hence if there exists a  $\beta' > 0$  such that  $k \phi k_{L^2(\gamma)} \cdot k^{\beta'}$ , then Assumption 2.4(ii) holds.

*Proof.* Noting the Definition (1.21) of  $M_Z(u)$ , we bound each of the three components separately.

(i) Firstly, the bound on  $ku^{inc}_{BS} k_{L^\infty(\Omega_+ \setminus Z)}$ ,

$$\begin{aligned} \|u_{BS}^{inc}\|_{L^\infty(\Omega_+ \setminus Z)} &\lesssim \inf_{\mathbf{x} \in \Omega_+ \setminus Z} \int_\gamma \left| \frac{1}{(k|\mathbf{x} - \mathbf{y}|)^{1/2}} \varphi(\mathbf{y}) \right| ds(\mathbf{y}) \\ \|u_{BS}^{inc}\|_{L^\infty(\Omega_+ \setminus Z)} &\leq \inf_{\mathbf{x} \in \Omega_+ \setminus Z} \int_\gamma |\Phi(\mathbf{x}, \mathbf{y}) \varphi(\mathbf{y})| ds(\mathbf{y}) \end{aligned}$$

and using (A.7) we can bound

from which it follows that

$$ku^{inc}_{BS} k_{L^\infty(\Omega_+ \setminus Z)} \cdot k^{-1/2} k \phi k_{L^2(\gamma)}. \tag{1.25}$$

(ii) Secondly, the bound on  $ku^s k_{L^\infty(\Omega_+)}$ . We start by rewriting the  $k$ -weighted norm

$$\begin{aligned} \|u_{BS}^{inc}\|_{H^1_k(\Omega_+)} &= \left( \int_\Gamma k^2 |u_{BS}^{inc}|^2 + |\nabla_\Gamma u_{BS}^{inc}|^2 ds \right)^{1/2} \\ &= \left( \int_\Gamma k^2 |\mathcal{S}_{\gamma \rightarrow \Gamma} \varphi|^2 + |\mathcal{D}_{\gamma \rightarrow \Gamma} \varphi|^2 ds \right)^{1/2} \\ &\lesssim (k \|\mathcal{S}\|_{L^2(\gamma) \rightarrow L^2(\Gamma)} + \|\mathcal{D}\|_{L^2(\gamma) \rightarrow L^2(\Gamma)}) \|\varphi\|_{L^2(\gamma)}. \end{aligned}$$

We may bound further using Lemma 5.14(i) and (ii), to obtain

$$ku^{inc}_{BS} k_{H^1_k(\Omega_+)} \cdot (k^{1/2} + 1) k \phi k_{L^2(\gamma)},$$

which when combined with Theorem 1.1(ii) yields

$$ku^s k_{L^\infty(\Omega_+)} \cdot \log^{1/2} k k \phi k_{L^2(\gamma)}, \tag{1.26}$$

for  $k \geq k_0$ .

(iii) Thirdly, the bound on  $ku^{inc}_{BS} k_{L(Z)}$ . Using the definition (1.11) of the  $L(Z)$  norm, we may write

$$\begin{aligned} \sup_{c, \theta} \left( \int_{\ell_{c, \theta} \cap Z} |u_{BS}^{inc}|^2 ds \right)^{1/2} &= \sup_{c, \theta} \left( \int_{\ell_{c, \theta} \cap Z} \left| \int_\gamma \Phi(\mathbf{x}, \mathbf{y}) \varphi(\mathbf{y}) ds(\mathbf{y}) \right|^2 ds(\mathbf{x}) \right)^{1/2} \\ &\leq \sup_{c, \theta} \left( \int_{\ell_{c, \theta} \cap Z} \left( \int_\gamma \frac{1}{4} \sqrt{\frac{2}{k\pi|\mathbf{x} - \mathbf{y}|}} |\varphi(\mathbf{y})| ds(\mathbf{y}) \right)^2 ds(\mathbf{x}) \right)^{1/2} \end{aligned}$$

using the bound on the Hankel function (A.7) once more. It then follows by [7, Lemma 1.2(a)] that

$$k \text{incBSkL}(Z) \cdot k^{-1/2} \phi k L^2(\gamma). \tag{1.27}$$

Combining (1.25)-(1.27) with the definition (1.21) yields the result for  $M_Z(u)$ . The result for  $M_\infty(u)$  follows by taking the limit as the region  $Z$  shrinks towards a set of measure zero.

We note that Theorems 1.11 and 1.12 imply  $M(u) = M_Z(u) \cdot \log^{1/2} k$  for sufficiently large  $k$ , which is sharper in its  $k$ -dependence than the plane wave case of Remark for which the corresponding bound is  $M(u) = M_\infty(u) \cdot k^{1/2} \log^{1/2} k$ . It should be noted that this bound is not believed to be sharp, as numerical experiments suggest  $M(u) = O(1)$  for plane wave incidence (see [35, §6]). These theorems, coupled with Theorem 1.10 show that Assumption holds for the point source and beam source incidence, therefore exponential convergence of the HNA method.

### VII. ALGEBRAIC EXPERIMENTATIONS FOR THE POINT SOURCE

We now establish via numerical examples the effectiveness of the Hybrid Numerical Asymptotic method for the point source problem. Specifically we consider the problems where  $\Omega$  is an equilateral triangle ( $n_\Gamma = 3$ ) with  $L_j = 2\pi$  for  $j = 1, \dots, n_\Gamma$ , with incident field  $u^{\text{inc}}_{PS}(\mathbf{x}; \mathbf{s})$  for a range of  $\mathbf{s}$  which will be introduced shortly. Figure 1.10 plots the approximation  $u$  to both problems, whilst Figure 1.12 plots the boundary solution  $v_p$  of for the triangle and regular pentagon ( $n_\Gamma = 5$ ). In both cases the absolute value of the boundary solution is largest at the point of the boundary which is closest to the source. This is largely accounted for by the geometrical optics component  $\Psi_{PS}$ . We solve using the classical combined formulation using the Galerkin method outlined on a single mesh, hence we seek  $v_N \in \overline{V}_N^{\text{HNA}}(\Gamma)$  such that

$$(\mathcal{A}_{k,\eta} v_N, \varphi)_{L^2(\Gamma)} = \frac{1}{k} (f - \mathcal{A}_{k,\eta} \Psi_{PS}, \varphi)_{L^2(\Gamma)}, \quad \text{for all } \varphi \in \overline{V}_N^{\text{HNA}}(\Gamma), \tag{1.28}$$

where  $\Psi_{PS}$  is as in (1.13). For the mesh parameters. we introduce some polynomial dependence on  $\alpha_j$ , choosing  $\alpha_j = \min((1 + (\mathbf{p}_j)_i)/8, 2)$ , where  $i$  corresponds to the  $i$ th mesh element on the  $j$ th side. The result of Theorem still holds, given that  $\alpha_j$  is bounded above by a constant independent of the polynomial degree. We choose  $c_j = 2$ , and we choose the polynomial degree vectors  $\mathbf{p}_j$  in accordance with Remark. We compute all inner products in the Galerkin method using the quadrature routines discussed in Appendix B. We note also that the set  $Z$  discussed throughout this section is not a parameter of the numerical method; we require only that such a  $Z$  exists. Convergence analysis was run for  $k \in \{5, 10, 20, 40, 80, 160\}$  with  $p \in \{1, \dots, 7\}$ , taking  $p = 8$  as the reference solution. The approximation was also validated by means of comparison against a standard BEM solution, we do not give these results here. For the triangle, the vertices are

$$\mathbf{P}_1 = \begin{pmatrix} 2\pi/\sqrt{3} \\ 0 \end{pmatrix}, \quad \mathbf{P}_2 = \begin{pmatrix} -\pi/\sqrt{3} \\ \pi \end{pmatrix}, \quad \mathbf{P}_3 = \begin{pmatrix} -\pi/\sqrt{3} \\ -\pi \end{pmatrix},$$

whilst the point sources we consider are emanating from

$$\mathbf{s}_1 = \begin{pmatrix} 1 \\ 4 \end{pmatrix}, \quad \mathbf{s}_2 = \begin{pmatrix} 4 \\ 0 \end{pmatrix}, \quad \mathbf{s}_3 = \begin{pmatrix} -\pi/\sqrt{3} \\ -4 \end{pmatrix}.$$

Figures 1.8 and 1.9 show the convergence of the HNA Galerkin method for each of the three cases for the triangle, which are depicted in Figure (1.7). In each case

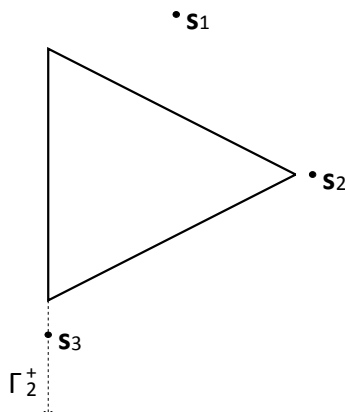


Figure 1.7: Schematic of triangular scatterer  $\Omega$  with position of each source point

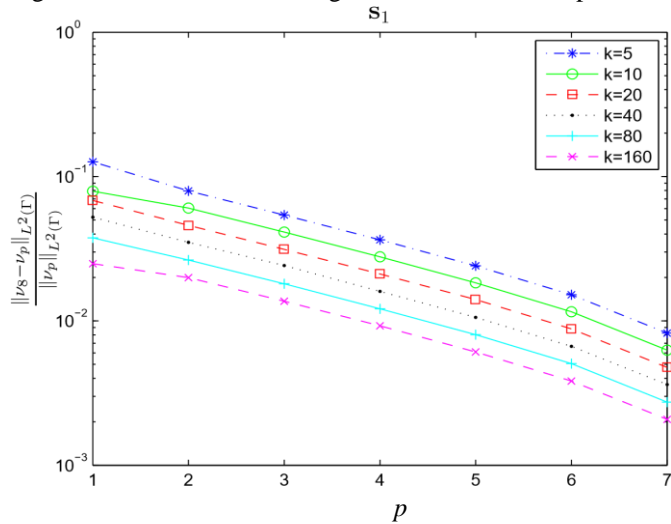
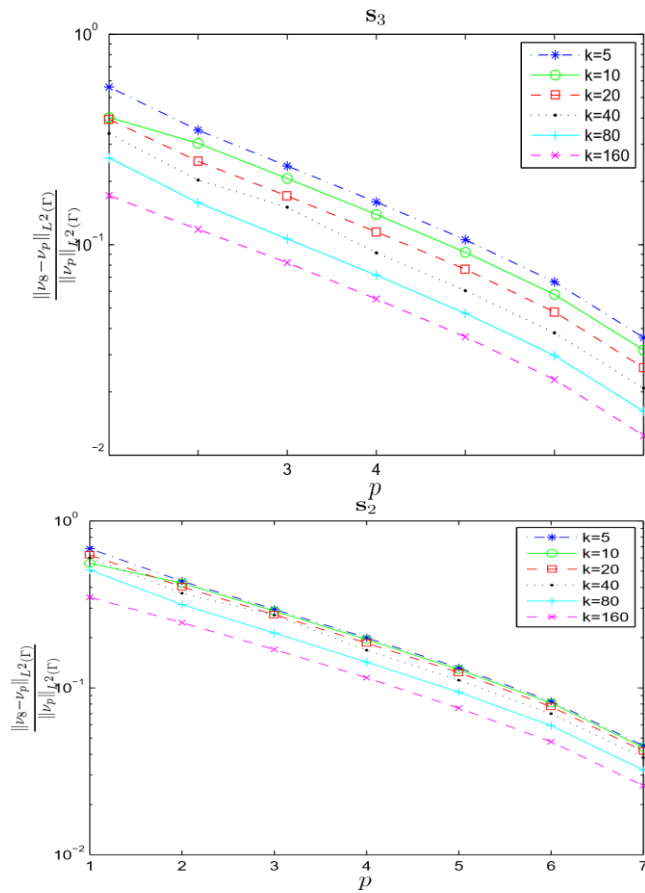


Figure 1.8: Relative  $L^2(\Gamma)$  errors for the triangle, for source point  $s_1$ .



Relative  $L^2(\Gamma)$  errors for the triangle, for source point  $s_2$  and  $s_1$ .

Figure 1.9:

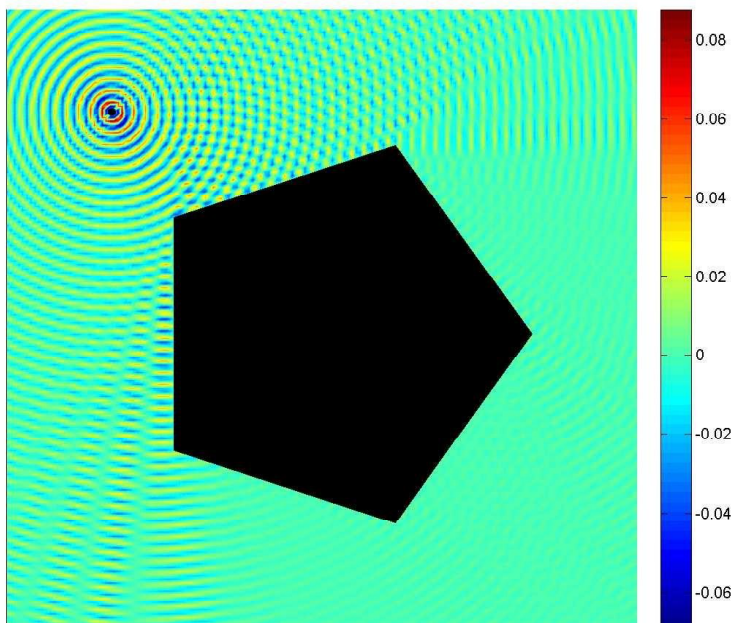
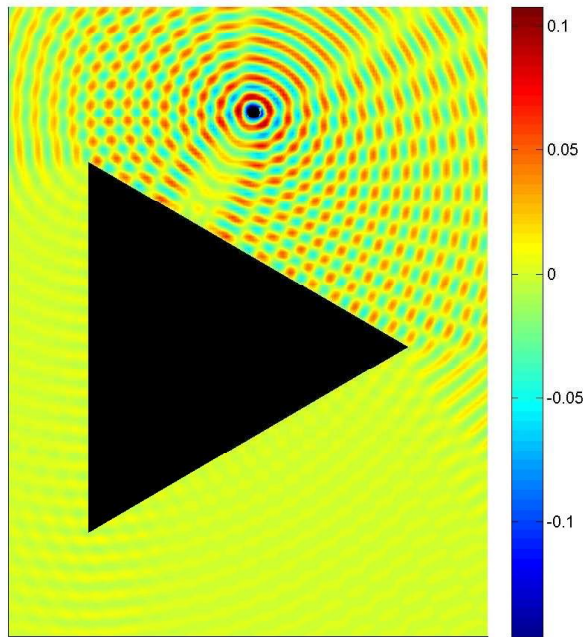


Figure 1.10: Real part of  $u_N$  for  $p = 8$  in  $\Omega_+$  for the regular triangle and the pentagon, with wavenumber  $k = 20$ . The source point  $\mathbf{s}$  is covered by a set  $Z = B_{1/k}(\mathbf{s})$  inside which we do not evaluate  $u$ . This was done for aesthetic reasons; the colourbar scale would be skewed for large values of  $\Phi(\mathbf{x}, \mathbf{s})$ , when  $\mathbf{x}$  is close to  $\mathbf{s}$ .

we observe similar rates of exponential convergence. Moreover, for fixed  $p$  the error does not increase with  $k$ , indeed it can be seen to decrease, which demonstrates the frequency independence of our approach. For a source point  $\mathbf{s}_1$ , we observe the lowest relative errors, which can be explained as the source is furthest away from  $\Omega_-$  in this case. Theorem (1.11) suggests that  $M_Z(u)$  of (1.21) grows with  $1/\text{pdist}(\mathbf{s}, \Omega_-)$ . The point  $\mathbf{s}_2$  is closer to  $\Omega_-$  than  $\mathbf{s}_1$ , with distance  $|\mathbf{s}_2 - \mathbf{P}_1| \approx 0.372$ , for which the rate of convergence appears to be shifted by a multiplicative constant which further justifies the hypothesis that

convergence is weaker for source point closer to  $\Gamma$ . The point  $\mathbf{s}_3$  was chosen to lie on the extended line  $\Gamma^+$ , such that the integrand of (1.2) is unbounded, as the path of integration contains a singularity. This confirms the theoretical result that the HNA method will converge exponentially, even if the solution  $u$  is unbounded on the extended line (as previous analyses of HNA methods would not explain this). The method can be seen to converge similarly for  $\mathbf{s}_3$ , which is to be expected given the distance is  $|\mathbf{s}_3 - \mathbf{P}_3| \approx 0.858$ ,  $\mathbf{s}_3$  is a similar distance from  $\Omega$ - as  $\mathbf{s}_2$ . Figure 1.11 shows how the conditioning of the discrete system grows with  $p$  and  $k$ . Recall from that the conditioning of the discrete system depends closely on the choice of  $\alpha_j$ , which here is chosen to be  $\min((1+(\mathbf{p}_j)/8), 2)$ . It is difficult to determine trends in the conditioning from this plot, for lower wavenumbers  $k = 5, 20, 40$  the conditioning appears to peak, and then drop for higher  $p$ . If poor conditioning causes the system to become unstable, a larger value of  $\alpha_j$  should be chosen, removing unnecessary basis elements. This can be done without computation of any further inner products; carefully selected rows and columns from the discrete system can be removed to achieve this. Implementation of the beam source problem follows similarly, although we do not present any results here. In such a case, the right hand side will contain a triple integral  $(A\Psi_{BS}, \varphi)_{L^2(\Gamma)}$  for basis function  $\varphi$ , as in this instance  $\Psi_{BS}$  itself contains an integral.

**VIII. CONCLUSIONS AND FURTHER WORK**

In this paper we have developed theory that proves the HNA method converges exponentially for Herglotz-type, point and beam source incidence. This was demonstrated by numerical examples for the case of the point source. A key development for future work is to generalise the density of the beam source term to  $H^{-1/2}(\gamma)$ , rather than  $H^{-1/2+\varrho}(\gamma)$  for  $\varrho > 0$  that has been explored here. This would be essential for analysis of iterative HNA methods for multiple screen

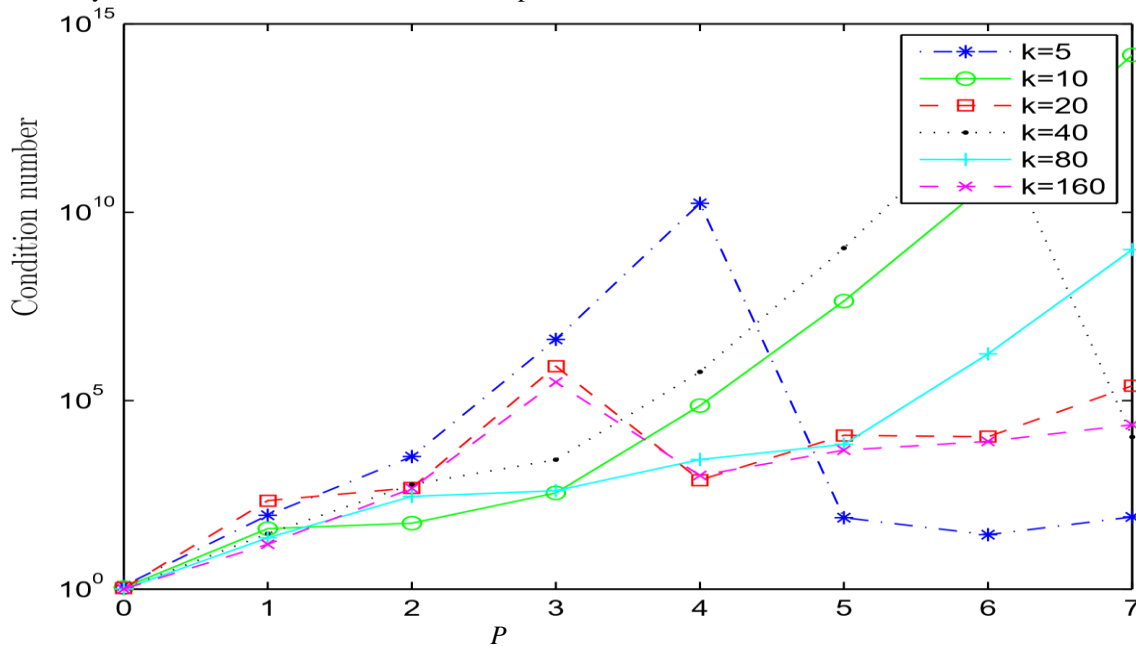
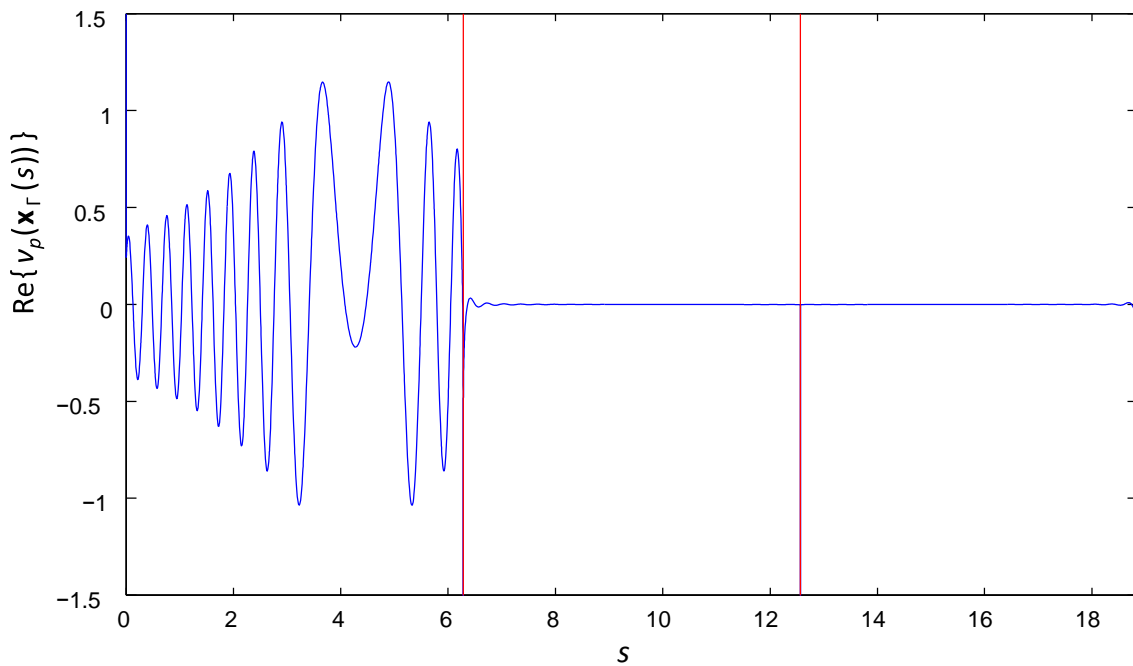
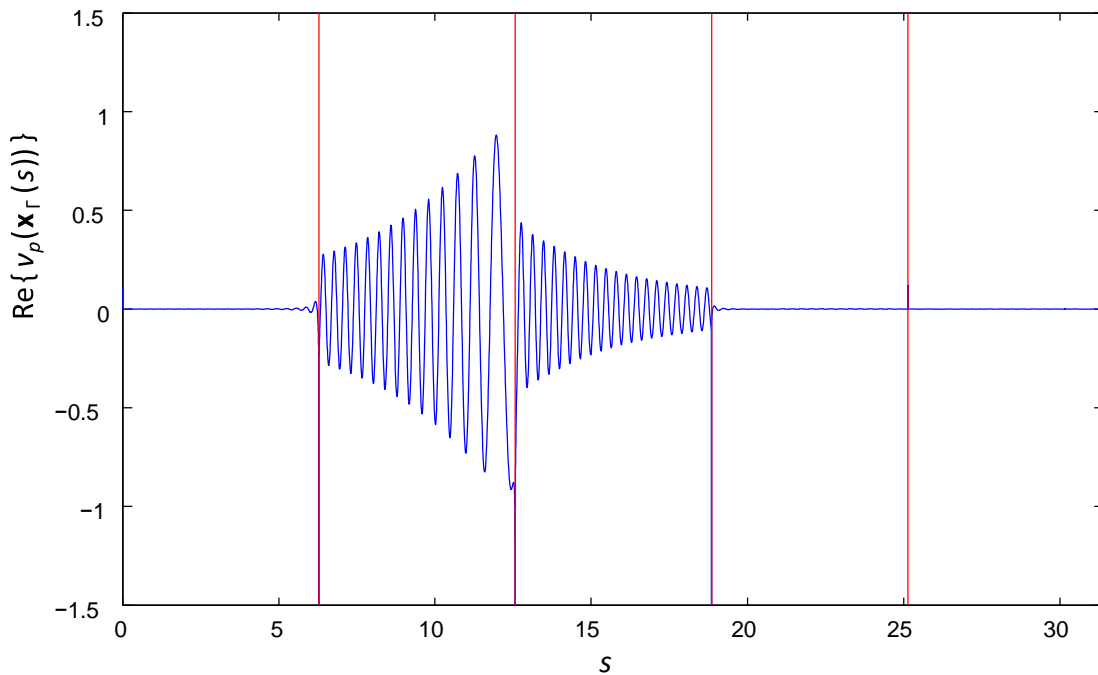


Figure 1.11: Plot of condition number of Galerkin matrices against  $k$  and  $p$ , for the triangle problem.



(a)



(b) Figure 1.12: Plot of real part of boundary solution, for the problems depicted in Figure 1.10 (a) and (b). problems, which we plan to address in future work. Alternatively, the methods in this paper may be combined with non-convex polygons of the penetrable obstacles.

## REFERENCES

- [1] Jean-Claude Nédélec. *Acoustic and electromagnetic equations*, volume 144 of *Applied Mathematical Sciences*. Springer-Verlag, New York, 2001. Integral representations for harmonic problems.
- [2] S. Nonnenmacher and M. Zworski. Quantum decay rates in chaotic scattering. *Acta. Math.*, 203(2):149–233, 2009.
- [3] E. Parolin. A hybrid numerical-asymptotic boundary element method for highfrequency wave scattering. Master’s thesis, University of Oxford, 2015.
- [4] A. Quarteroni and A. Valli. *Numerical approximation of partial differential equations*, volume 21. Springer Science & Business Media, 2008.

- [5] S. A. Sauter and C. Schwab. *Boundary element methods*. Springer, 2010.
- [6] E. A. Spence. Wavenumber-explicit bounds in time-harmonic acoustic scattering. *SIAM J. Math. Anal.*, 46(4):2987–3024, 2014.
- [7] E. A. Spence. “When all else fails, integrate by parts” - an overview of new and old variational formulations for linear elliptic PDEs, chapter 6. SIAM, 2015. Author’s personal copy available at: <http://people.bath.ac.uk/eas25/ibps.pdf>, any numbered theorems, equations etc. inside of this thesis are referring to this version.
- [8] E. A. Spence, S. N. Chandler-Wilde, I. G. Graham, and V. P. Smyshlyaev. A new frequency-uniform coercive boundary integral equation for acoustic scattering. *Comm. Pure Appl. Math.*, 64(10):1384–1415, 2011.
- [9] E. A. Spence, I. V. Kamotski, and V. P. Smyshlyaev. Coercivity of combined boundary integral equations in high-frequency scattering. *Communications on Pure and Applied Mathematics*, 68(9):1587–1639, 2015.
- [10] O. Steinbach. *Numerical approximation methods for elliptic boundary value problems: finite and boundary elements*. Springer Science & Business Media, 2007.
- [11] P. C. Waterman. New formulation of acoustic scattering. *J. Acoust. Soc. Am.*, 45(6):1417–1429, 1969.
- [12] W. J. Wiscombe. Improved Mie scattering algorithms. *Appl. Optics*, 19(9):1505–1509, 1980.
- [13] Jared Wunsch. Resolvent estimates with mild trapping. *J. E. D. P.*, pages 1–15, 201